Acta Pharmaceutica Sinica B 2020;10(9):1658−1668

Chinese Pharmaceutical Association
Institute of Materia Medica, Chinese Academy of Medical Sciences

Acta Pharmaceutica Sinica B

www.elsevier.com/locate/apsb
www.sciencedirect.com

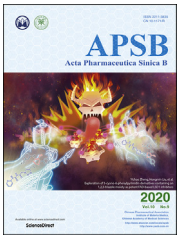

ORIGINAL ARTICLE

Exploration of 5-cyano-6-phenylpyrimidin derivatives containing an 1,2,3-triazole moiety as potent FAD-based LSD1 inhibitors

Liying Ma[†], Haojie Wang[†], Yinghua You, Chaoya Ma, Yuejiao Liu, Feifei Yang, Yichao Zheng[*], Hongmin Liu[*]

Collaborative Innovation Center of New Drug Research and Safety Evaluation, Henan Province; Key Laboratory of Technology of Drug Preparation (Zhengzhou University), Ministry of Education of China; Key Laboratory of Henan Province for Drug Quality and Evaluation; School of Pharmaceutical Sciences, Zhengzhou University, Zhengzhou 450001, China

Received 18 December 2019; received in revised form 24 January 2020; accepted 7 February 2020

KEY WORDS

LSD1 inhibitors;
Pyrimidine;
Anticancer;
Flavin adenine dinucleotide (FAD);
Gastric cancer

Abstract Histone lysine specific demethylase 1 (LSD1) has become a potential therapeutic target for the treatment of cancer. Discovery and develop novel and potent LSD1 inhibitors is a challenge, although several of them have already entered into clinical trials. Herein, for the first time, we reported the discovery of a series of 5-cyano-6-phenylpyrimidine derivatives as LSD1 inhibitors using flavin adenine dinucleotide (FAD) similarity-based designing strategy, of which compound **14q** was finally identified to repress LSD1 with IC_{50} = 183 nmol/L. Docking analysis suggested that compound **14q** fitted well into the FAD-binding pocket. Further mechanism studies showed that compound **14q** may inhibit LSD1 activity competitively by occupying the FAD binding sites of LSD1 and inhibit cell migration and invasion by reversing epithelial to mesenchymal transition (EMT). Overall, these findings showed that compound **14q** is a suitable candidate for further development of novel FAD similarity-based LSD1 inhibitors.

Abbreviations: AML, acute myeloid leukemia; EMT, epithelial to mesenchymal transition; ESI, electrospray ionization; FAD, flavin adenine dinucleotide; FBS, fetal bovine serum; HRMS, high resolution mass spectra; IC_{50}, half maximal inhibitory concentration; LSD1, histone lysine specific demethylase 1; MOE, molecular operating environment; ANOVA, analysis of variance; PAINS, pan assay interference compounds; PDB, the Protein Data Bank; RLU, relative light units; SARs, structure−activity relationship studies; TCP, tranylcypromine; VDW, van der Waals.

*Corresponding authors. Tel./fax: +86 371 67781739.
E-mail addresses: yichaozheng@zzu.edu.cn (Yichao Zheng), liuhm@zzu.edu.cn (Hongmin Liu).
[†]These authors made equal contributions to this work.

Peer review under responsibility of Institute of Materia Medica, Chinese Academy of Medical Sciences and Chinese Pharmaceutical Association

https://doi.org/10.1016/j.apsb.2020.02.006

1. Introduction

Epigenetic plays a key role in life and controls gene expression and transcription, and contributes to a variety of cellular processes, including cell differentiation, proliferation and migration[1,2]. Among the diverse epigenetic modifiers, histone lysine specific demethylase 1 (LSD1), the first identified histone demethylase, specifically removes the methyl groups from mono- and di-methylated H3K4 and H3K9 *via* enzymatic oxidation, and contributes to the downstream gene transcription[3−7]. As reported, LSD1 is overexpressed in many human cancers, such as gastric cancer, lung cancer, leukemia, etc., and abrogation of LSD1 leads to the anticancer effect[8−16], which suggests LSD1 as a promising therapeutic target for cancer.

Signficant efforts have been made to develop biological active LSD1 inhibitors over the past decade[4,17−29]. So far, six tranylcypromine (TCP)-based LSD1 inhibitors have already advanced into clinic trials for the treatment of acute myeloid leukemia (AML) as well as small-cell lung cancer, including GSK2879552, INCB059872, ORY-2001, ORY-1001, CC-90011 and IMG-7289[30−34]. In addition to TCP-based inhibitors, multiple LSD1 inhibitors with diverse classes structures, such as polyamine-, peptide-, phenelzine-, pargyline- and triazole-based derivatives, have also been reported (Fig. 1). Nevertheless, most of these inhibitors still perform some shortages. For instance, TCP-based LSD1 inhibitors generally displayed some side effects due to irreversible binding with the endogenous flavin adenine dinucleotide (FAD) and micromolar affinity with many targets in body, such as norepinephrine transporter, dopamine transporter, etc[35,36]. Phenelzine- and pargyline-based derivatives displayed insufficient activities and poor selectivity[37,38]. Although Kumarasinghe et al.[39,40] reported that the weak cytotoxicity of peptide-based LSD1 inhibitors could be improved by lipidation, there are still few reported about inhibitors with excellent enzyme activity and cell activity. Thus, the discovery of potent and specific LSD1 inhibitor has become an urgent requirement.

As the cofactor of LSD1 is FAD[41,42], compounds with similar structure to FAD may compete with FAD for binding to LSD1, which may represent a promising approach to inhibit the activity of LSD1. In previous work, we have reported several new LSD1 inhibitors[8,29,43−52], among which 1,2,3-triazole-dithiocarbamate hybrids exhibited moderate inhibitory activity by competitively binding to LSD1. In an effort to design and develop novel and potent LSD1 inhibitors, we screened our in-house pyrimidine derivatives on LSD1 inhibitory activity. Fortunately, we found series I, compounds containing triazole unit, exhibited potent LSD1 inhibitory activity, and docking analysis revealed that they could inhibit LSD1 activity by competing the binding sites of FAD in LSD1. Subsequently, series II with improved LSD1 inhibitory activity were obtained by extending side chain to further increase the similarity between FAD and series I derivatives, and compound **14q** was finally identified to inhibit LSD1 with IC_{50} = 183 nmol/L in an FAD competitive manner and inhibit cell migration and invasion by reversing epithelial to mesenchymal transition (EMT, Scheme 1).

2. Results and discussion

2.1. Chemistry

Target compounds were synthesized using previously described procedures[51−53]. Scheme 2 displays the synthetic routes of the target compounds 5-cyano-6-phenyl-pyrimidine derivatives. Intermediates **4a**−**f** were obtained from reaction of benzaldehydes **1a**−**f** with ethyl cyanoacetate thiourea, and potassium carbonate in ethanol. Then, reaction of **4a**−**f** with propargyl bromide in dioxane afford **6a**−**f**. Compound **6a** reacted with different arylamines in ethanol at reflux led to **7a**−**g**. Compound **11** reacted with sodium azide, yielding compound **12**. Compounds **4a**−**d** were allowed to react with compound **11** to yield the target compounds **15a**−**d**. The intermediates **6a**−**f** with appropriate substituted benzyl azides and compounds **12** *via* click reaction generated the corresponding compounds **9a**−**f** and **13a**−**f**. Then, these intermediates (**9a**−**f**, **13a**−**f** and **15a**−**d**) were treated with corresponding arylamines in ethanol, affording compounds **10a**−**l**, **14a**−**w** and **16a**−**d**.

2.2. LSD1 inhibitory activity and structure−activity relationship studies (SARs)

The LSD1 inhibitory activity against of all synthesized compounds and a reference compound, GSK-LSD1, was examined[29]. The results are summarized in Tables 1−4. Besides, all compounds have passed the PAINS screening using the online program (http://www.cbligand.org/PAINS/)[54].

In previous work, we have found that the introduction of 1,2,3-triazole group could effectively improve the anti-proliferative activity of pyrimidine-based derivatives. Moreover, Holshouser et al.[55] and Kutz et al.[56] also reported a class of compounds containing 3,5-diamino-1,2,4-triazoles as novel inhibitors. Further mechanism studies found that compared with parent compounds **7a**−**g**, the introduction of 1,2,3-triazole moiety (**10a**−**g**) could effectively improve the inhibitory activity against LSD1 (Table 1). These findings suggest that 1,2,3-triazole group was benefit to the discovery of 5-cyano-6-phenylpyrimidine-based LSD1 inhibitors.

To explore the correlation between the introduction of 1,2,3-triazole and the improvement of LSD1 inhibitory activity, the proposed binding modes of compound **10a** in LSD1 were analyzed using the Molecular Operating Environment (MOE, version 2015.10) package. The docking results indicated that compound **10a** fitted well into the FAD binding pocket of LSD1 (Fig. 2A). The triazole formed a hydrogen bond with Val288, and the cyano group connected to pyrimidine formed a key hydrogen bond with Lys661 bridged by water1032 as Lys661 is essential for LSD1 activity, which may form a hydrogen bond with the N5 atom of FAD *via* a conserved water molecule. In addition, the phenyl group connected with pyrimidine was found to be located in the hydrophobic pocket surrounded by Tyr761, Arg316, Lys661, Trp751 and Leu659, while the trifluoromethyl-benzene had hydrophobic interactions with Tyr761, Ala539, Thr810, Val811 and Val333 (Fig. 2B). These findings reveal that the introduction of 1,2,3-triazole may inhibit the activity of LSD1 by stabilizing the conformation of series I derivatives to compete with FAD in LSD1.

Based on the above findings, to further investigate the influence for increasing similarity of target compounds with FAD on LSD1 inhibitory activity, series II derivatives containing hydrogen bond donor and receptor groups between 1,2,3-triazole and pyridine ring were designed and synthesized. Their inhibitory activities were listed in Table 2. To our delight, compared with series I derivatives, compounds **14a**−**e** with the extension of the side chain exhibit stronger inhibitory activity against LSD1, suggesting that the increased activity of LSD1 may be related to their structural similarity to FAD. Particularly, compound **14e** displayed significantly increased inhibitory activity against LSD1 with the

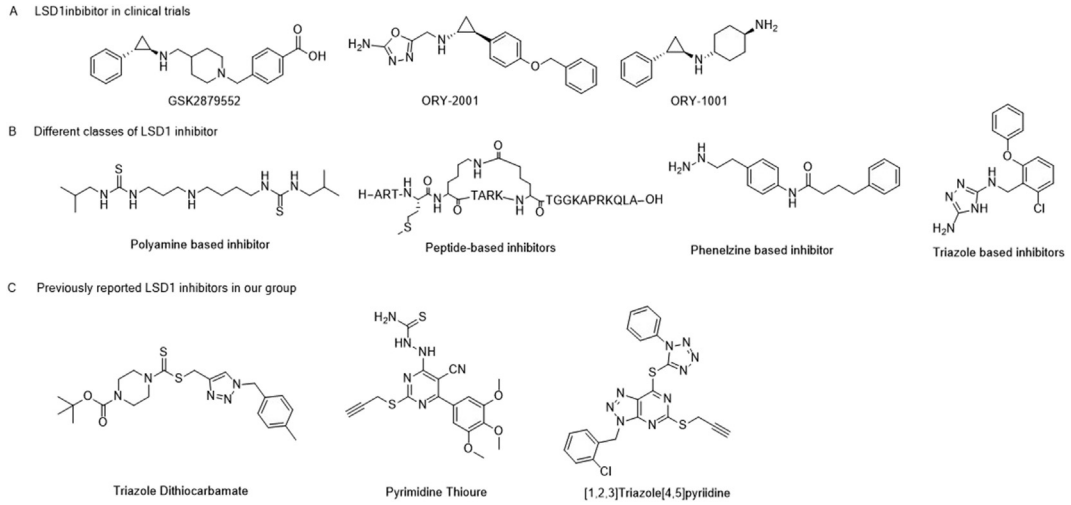

Figure 1 Representative examples of LSD1 inhibitor.

inhibitory rate of 89.2% at 1 μmol/L, about 50-fold more potent than of compound **10l**.

The exciting discovery prompted us to further explore the SARs of series II derivatives. Their inhibition results were summarized in Table 3. Majority of these compounds showed excellent activity with IC_{50} value ranging from 183 nmol/L to 5.62 μmol/L. The SARs found that in terms of the *para*-methyl substitution in R_2, compounds (**14b**, **14d** and **14e**) with an electron-withdrawing or -donating group in R_1 resulted in a similar inhibitory activity against LSD1 compared with compound **14a**. However, compound **14c** with *para*-chlorine and compound **14f** with *para*-isopropyl substitution in R_1 have significantly increased inhibitory activity, which were about 3.5- and 5-fold stronger than that of compound **14a**, respectively. These findings indicate that the types of substituents have a more significant effect on the activity than the electrical properties of substituents at R_1. Furthermore, except for compound **14j**, compounds **14g** and **14i** with *ortho*-electron-donating substitution displayed more potent activity than corresponding compound **14h** with electron-withdrawing group. Interestingly, compounds **14f**, **14l** and **14m** with *para*-substitution at aromatic ring in R_2, showed improved inhibitory activity against LSD1 compared with *ortho*-substituted analogue and unsubstituted aromatic ring in R_2, excitingly, except for compound **14n**. Compound **14p** with electron-withdrawing exhibited better activity compared to compounds **14b** and **14o**. In particular, the compound **14q** with *meta*-trifluoromethyl substituent at aromatic ring in R_2, exhibited remarkable inhibitory activity against LSD1 with an IC_{50} value of 183 nmol/L. It is worth noting that compounds **14n** and **14r** also showed excellent inhibitory activity, which is worthy of our further study of SARs. The IC_{50} values of compounds **14n** and **14r** against LSD1 are 287 and 387 nmol/L, respectively. Compound **14n**, with a *para*-methyl in R_1 and *para*-methoxy in R_2, showed better inhibitory activity compared with both its *para*-isopropyl in R_1 (**14m**) and *ortho*-methoxy in R_2 (**14o**) analogues. A similar trend was also observed (**14a**−**e**, **14g** *vs.* **14f**). The comparison of the influence of electronic-effect in compounds **14p**−**r** and **14v** on the LSD1 inhibitory activity is distinct. It reveals that simultaneous replacement of R_1 and R_2 (**14v**) with electron-withdrawing group resulted in a dramatically decreasing of LSD1 inhibitory activity, whereas replacement R_1 with electron-donating group and R_2 with electron-withdrawing exhibited excellent inhibitory activity. We also found that the electronic-effect on the activity of compounds **14c**, **14n**,

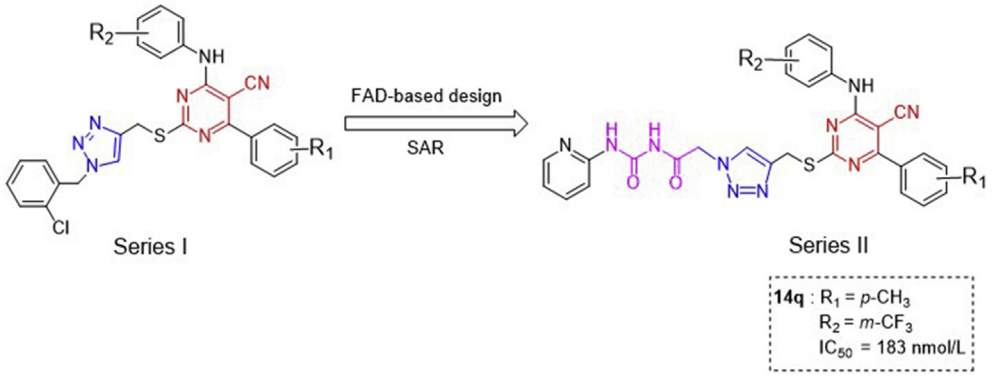

Scheme 1 Series II (**14q**) with the most potent inhibitory activity against LSD1 was obtained by FAD similarity-based designing strategy.

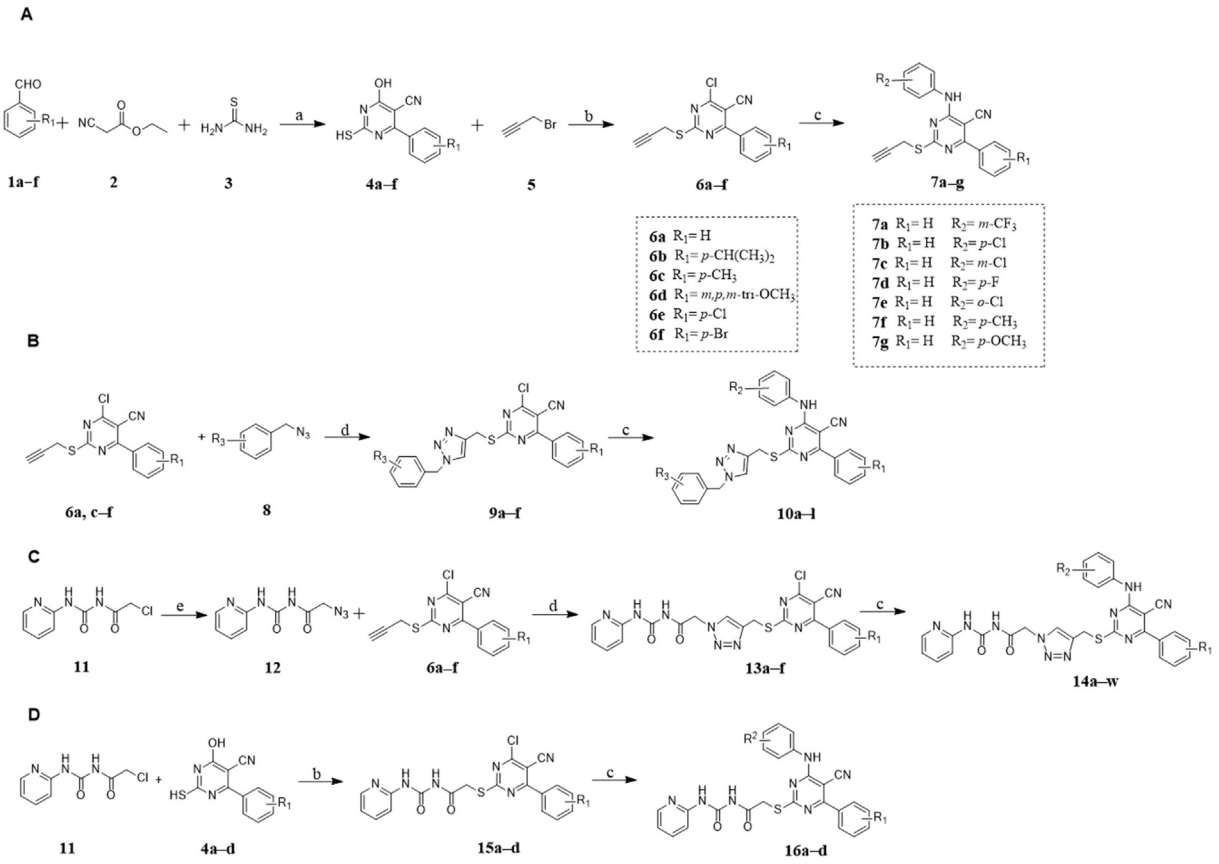

Scheme 2 Reagents and conditions: (a) EtOH, K_2CO_3, reflux, 5 h, 70%−85%; (b) (i) dioxane, reflux; (ii) $POCl_3$, reflux, 1 h; 45%−75% (two steps); (c) appropriate aniline, EtOH, reflux, 6 h, 70%−90%; (d) $CuSO_4 \cdot 5H_2O$, sodium ascorbate, THF/H_2O, 78%; (e) NaN_3, acetone/H_2O, 75%.

14q and **14r** is completely different, and we speculate that this result is due to the synergistic effect of the groups at two positions. In addition, compounds **14t** with *meta*-chlorine substitute at R_2 exhibited better inhibitory activity than corresponding compound **14s** with *para*-chlorine substitution. These results indicate that the substitution pattern and electronic-effect at R_2 are critical for inhibitory activity against LSD1. SAR was summarized and indicated in Fig. 3.

To further explore the effect of 1,2,3-triazole group activity, compounds **16a–d** were synthesized and evaluated on their LSD1 inhibitory activity. As shown in Table 4, compounds **16a−d** without 1,2,3-triazole moiety exhibited the complete loss of

Table 1 Inhibitory results of target compounds **7a–g** and **10a–g** against LSD1.

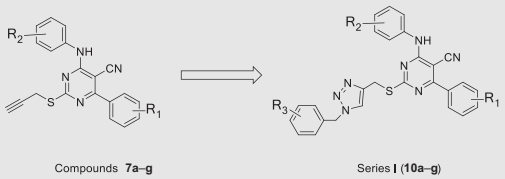

Compd.	R_1	R_2	IC_{50} (μmol/L)[a]	Compd.	R_1	R_2	R_3	IC_{50} (μmol/L)[a]
7a	H	*m*-CF_3	>64	**10a**	H	*m*-CF_3	*o*-Cl	0.407 ± 0.021
7b	H	*p*-Cl	>64	**10b**	H	*p*-Cl	*o*-Cl	0.628 ± 0.027
7c	H	*m*-Cl	>64	**10c**	H	*m*-Cl	*o*-Cl	6.310 ± 0.719
7d	H	*p*-F	>64	**10d**	H	*p*-F	*o*-Cl	3.227 ± 0.509
7e	H	*o*-Cl	>64	**10e**	H	*o*-Cl	*p*-CH_3	3.740 ± 0.573
7f	H	*p*-CH_3	>64	**10f**	H	*p*-CH_3	*p*-CH_3	40.408 ± 1.606
7g	H	*p*-OCH_3	>64	**10g**	H	*p*-OCH_3	*o*-Cl	1.433 ± 0.516

[a]Data are displayed as mean ± SD. All experiments were performed three times at least.

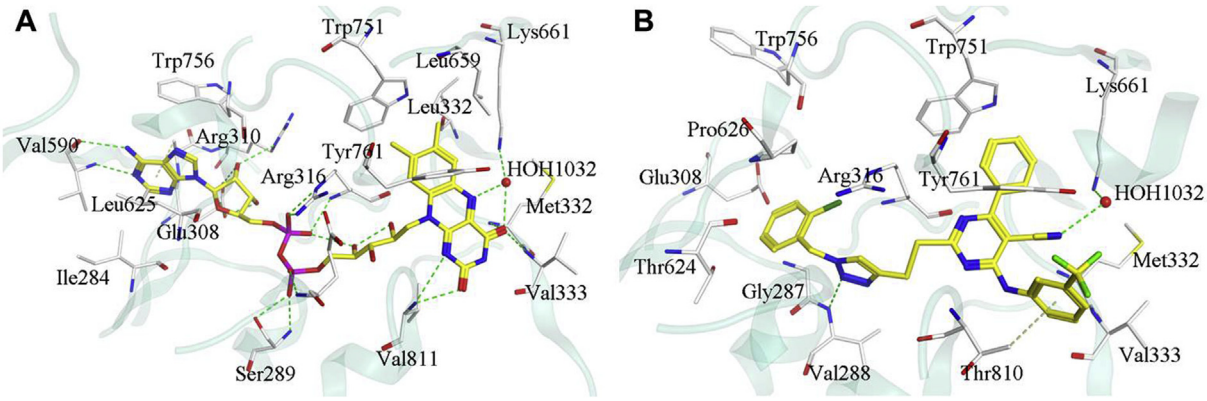

Figure 2 (A) The action mode of FAD (yellow) with LSD1 (PDB:2DW4); (B) the proposed binding mode of compound **10a** (yellow) in LSD1. Residues are shown as white lines, water is shown as red ball and H-bonds are depicted in green dotted line, respectively.

activity, which further indicated that 1,2,3-triazole is an essential moiety for LSD1 inhibitory activity.

2.3. *Molecular docking study*

The possible binding mode of compound **14q** in LSD1 was predicted using MOE. The docking results suggested that the most potent compound **14q** could be well docked into the FAD-binding pocket. Considering the detailed binding mode, we selected the top docking conformation based on the docking score and SARs in combination mode (Fig. 4A). Through the superposed conformation of compound **14q** and FAD with LSD1 (Fig. 4B), it was found that they performed similar modes of action, and compound **14q** fitted into the FAD-binding pocket appropriately. The cyano group connected with pyrimidine formed a key hydrogen bonding interaction with Lys661 bridged by water1032, meanwhile, this cyano group may also form a hydrogen bond with Met332. The triazole ring formed a hydrogen bond with Val288. For bisamide moiety, the nitrogen and oxygen formed two hydrogen bonds with Thr624 and Arg316. Additionally, compound **14q** formed extensive van der Waals (VDW) interactions and hydrophobic interactions. The benzyl group connected with pyrimidine located in the hydrophobic pocket surrounded by Tyr761, Leu659, Lys661, Trp751 and the side chain of Arg316, while having a face to face π–π stacking with Tyr761 and Trp751. The trifluoromethyl-benzene group formed hydrophobic interactions with Tyr761, Ala539, Thr810, Val811 and Val333, and the

Table 2 Inhibitory activity of target compounds against LSD1.

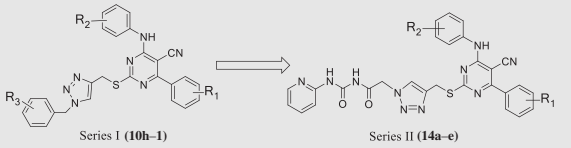

Compd.	R_1	R_2	R_3	Inhibition rate (%) at 1 μmol/L[a]
10h	H	*p*-CH_3	*o*-Cl	21.3
14a	H	*p*-CH_3		100
10i	*p*-CH_3	*p*-CH_3	*o*-Cl	83.7
14b	*p*-CH_3	*p*-CH_3		94.8
10j	*p*-Cl	*p*-CH_3	*o*-Cl	39.8
14c	*p*-Cl	*p*-CH_3		91.4
10k	*p*-Br	*p*-CH_3	*o*-Cl	8.4
14d	*p*-Br	*p*-CH_3		46.3
10l	*m,p,m*-tri-OCH_3	*p*-CH_3	*o*-Cl	2.2
14e	*m,p,m*-tri-OCH_3	*p*-CH_3		89.2

[a]All experiments were performed three times at least.

Table 3 Inhibitory results of target compounds **14a–w** against LSD1.

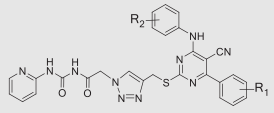

Compd.	R_1	R_2	IC_{50} (μmol/L)[a]
14a	H	*p*-CH_3	1.880 ± 0.272
14b	*p*-CH_3	*p*-CH_3	1.435 ± 0.150
14c	*p*-Cl	*p*-CH_3	0.531 ± 0.002
14d	*p*-Br	*p*-CH_3	3.822 ± 0.582
14e	*m,p,m*-tri-OCH_3	*p*-CH_3	1.262 ± 0.100
14f	*p*-$CH(CH_3)_2$	*p*-CH_3	0.384 ± 0.002
14g	p-$CH(CH_3)_2$	*o*-CH_3	3.822 ± 0.582
14h	*p*-$CH(CH_3)_2$	*o*-Cl	>10
14i	*p*-$CH(CH_3)_2$	*o*-OH	5.041 ± 0.702
14j	*p*-$CH(CH_3)_2$	*o*-OCH_3	>10
14k	*p*-$CH(CH_3)_2$	H	>10
14l	*p*-$CH(CH_3)_2$	*p*-F	5.620 ± 0.751
14m	*p*-$CH(CH_3)_2$	*p*-OCH_3	0.611 ± 0.215
14n	*p*-CH_3	*p*-OCH_3	0.287 ± 0.002
14o	*p*-CH_3	*o*-OCH_3	1.533 ± 0.271
14p	*p*-CH_3	*m*-Cl	0.232 ± 0.002
14q	*p*-CH_3	*m*-CF_3	0.183 ± 0.003
14r	*m,p,m*-tri-OCH_3	*m*-CF_3	0.387 ± 0.002
14s	*m,p,m*-tri-OCH_3	*p*-Cl	0.965 ± 0.003
14t	*m,p,m*-tri-OCH_3	*m*-Cl	0.635 ± 0.190
14u	*p*-Cl	*p*-$CH(CH_3)_2$	1.234 ± 0.091
14v	*p*-Br	*m*-CF_3	>10
14w	*p*-Br	*p*-$CH(CH_3)_2$	1.351 ± 0.130
GSK-LSD1	–	–	0.022 ± 0.0008

[a]Data are displayed as mean ± S.D. All experiments were performed three times at least. –Not applicable.

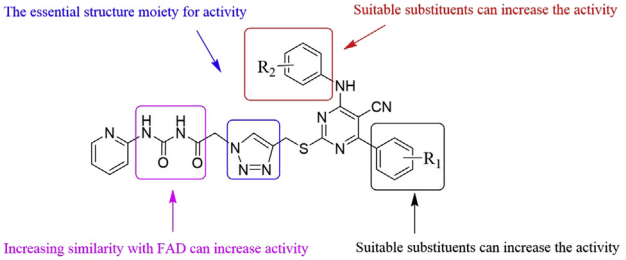

Figure 3 SAR for LSD1 inhibitory activity of series II.

Table 4 Inhibitory results of compounds **14a–d** against LSD1.

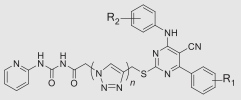

Compd.	R_1	R_2	*n*	IC_{50} (μmol/L)[a]
16a	H	*p*-CH_3	0	>125
14a	H	*p*-CH_3	1	1.881 ± 0.272
16b	*p*-$CH(CH_3)_2$	*p*-CH_3	0	>125
14f	*p*-$CH(CH_3)_2$	*p*-CH_3	1	0.384 ± 0.002
16c	*m,p,m*-tri-OCH_3	*m*-CF_3	0	>125
14r	*m,p,m*-tri-OCH_3	*m*-CF_3	1	0.387 ± 0.002
16d	*p*-CH_3	*m*-CF_3	0	>125
14q	*p*-CH_3	*m*-CF_3	1	0.183 ± 0.003

[a]Data are displayed as mean ± S.D. All experiments were performed three times at least.

pyridine performed hydrophobic interactions with Trp756, Val590, Ile284, Val629 and Leu625. All these interactions stabilized the binding conformation of compound **14q** with LSD1.

2.4. *Compound **14q** inhibits LSD1 selectively and competitively in a time dependent and reversible manner*

As compound **14q** was identified to inhibit LSD1 potently, selectivity of compound **14q** against homologous proteins of LSD1 remains to be answered. Hence, compound **14q** was subjected to MAO-A/B assay, and results indicated that compound **14q** cannot inhibit MAO-A/B (inhibitory rate against MAO-A/B less than 5% at 100 μmol/L), suggesting that compound **14q** is a selective LSD1 inhibitor. After that, further mechanism study was carried out to reveal the potential binding manner of compound **14q** against LSD1 recombinant. Firstly, dialysis experiment was carried out to investigate whether compound **14q** may bind to LSD1 recombinant in a reversible manner or irreversible manner. As indicated in Fig. 5A, compound **14q** may inhibit LSD1 in a reversible manner as dialysis mediated depletion of compound **14q** can rescue the activity of LSD1. To further confirm this result, centrifuge experiment and dilution assay were also carried out. With the aid of 10 kDa ultracentrifuge filter, reversible compound was supposed to be removed from LSD1 by centrifuge. So, compound **14q** was characterized as a reversible LSD1 inhibitor as split of compound **14q** by ultracentrifuge may rescue the activity of LSD1 either (Fig. 5B). And 80-fold dilution of compound **14q**/LSD1 mixture, which led to the lower concentration of compound **14q** in the enzyme reaction system, also resulted in the recovery of LSD1 enzymatic activity (Fig. 5C), indicating that compound **14q** was a reversible LSD1 inhibitor as proved by Fig. 5A and B. Then, time-dependent assay was also performed, and results showed that compound **14q** inhibited LSD1 in a time dependent manner (Fig. 5D). As compound **14q** could well penetrate into the FAD-binding pocket of LSD1, classic Lineweaver−Burk plots[55,57] was applied and results showed that compound **14q** was a competitive LSD1 inhibitor against FAD (Fig. 5E). Further recombinant-based thermal shift assay firmed that compound **14q** can stabilize LSD1 dose dependently (Fig. 5F), which suggests that compound **14q** can bind to LSD1 directly.

2.5. *Compound **14q** can inhibit LSD1 and reverse EMT cells*

As compound **14q** was confirmed as an FAD competitive LSD1 inhibitor in recombinant level, its cellular activity was further investigated in MGC-803 cell line, the one we chose previously[8]. First of all, cell viability was investigated when cells were treated with compound **14q** for 5 days, and results indicated that compound **14q** could inhibit the proliferation of MGC-803 cells with IC_{50} = 6.623 ± 0.359 μmol/L. Then, further cellular thermal shift assay was applied to confirm the target engagement of compound **14q** in cells. Result in Fig. 6A clearly suggested that compound **14q** enhanced the thermal stability of cellular LSD1 protein,

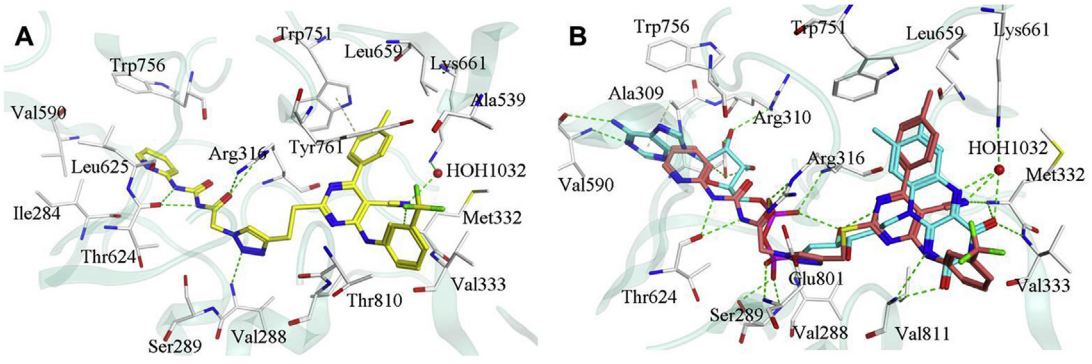

Figure 4 (A) The proposed binding mode of compound **14q** (yellow) in LSD1 (PDB:2DW4). The residues, water and H-bonds are shown in white lines, red ball and green dotted line, respectively. (B) The superposed conformation of compound **14q** (magenta sticks) and FAD (blue sticks) with LSD1.

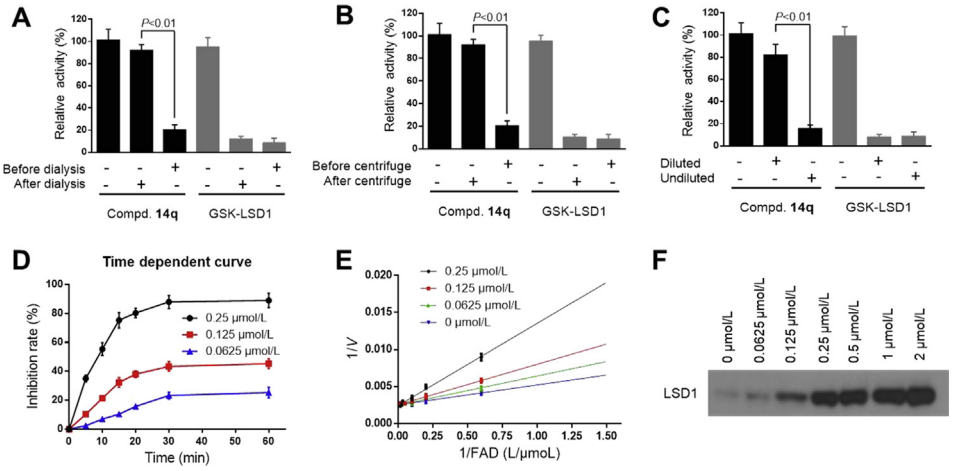

Figure 5 Mechanism study of compound **14q** on LSD1 inhibitory activity. (A)–(C) Reversible experiment of compound **14q** against LSD1 with dialysis experiments (A), ultrafiltration experiment (B) and dilution assay (C), GSK-LSD1 was used as a positive control; (D) compound **14q** can inhibit LSD1 in a time-dependent manner; (E) Lineweaver−Burk plots demonstrated that compound **14q** was a competitive inhibitor against FAD; (F) enhancement of thermal stability of LSD1 in the presence of compound **14q**. LSD1 protein was treated with compound **14q** for 1 h, followed by heating at 53 °C for 3 min. Data are displayed as mean ± SD. All experiments were performed three times at least. $^{*}P < 0.05$, $^{**}P < 0.01$.

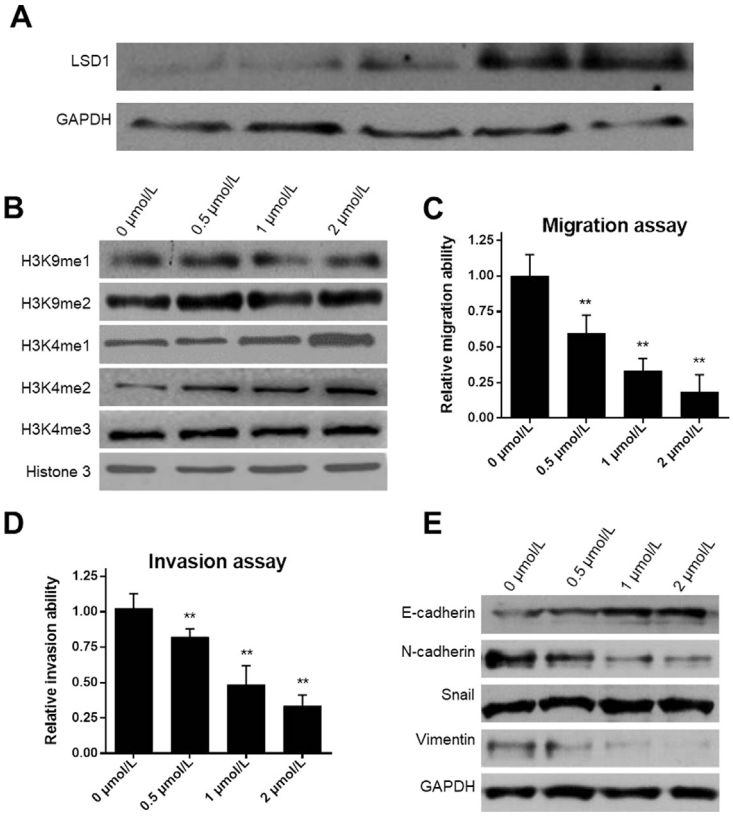

Figure 6 LSD1 inhibitory activity of compound **14q** in MGC-803. (A) Cellular based thermo stability assay of LSD1 in MGC-803 cells with the treatment of indicated concentrations of compound **14q**; (B) accumulation of H3K4me1/2/3 and H3K9me1/2 with indicated treatment for 5 days; (C) and (D) compound **14q** treatment led to the inhibition of migration (C) and invasion (D) ability in MGC-803 cells; (E) amount of E-cadherin, N-cadherin, Snail and vimentin after compound **14q** treatment for 24 h. Data are displayed as mean ± S.D. All experiments were performed three times at least. $^{*}P < 0.05$, $^{**}P < 0.01$.

indicating cellular target engagement of compound **14q** in MGC-803 cells. To determine the inhibitory effect of our compound against LSD1 in cells, amount of four reported LSD1 substrates H3K4me1/2 and H3K9me1/2 were analyzed as well as H3K4me3, a substrate of JMJC containing demethylase. As shown in Fig. 6B, the amount of H3K4me1 and H3K4me2 showed a dose-dependent accumulation in the presence of compound **14q** for 5 days, while expressions of H3K9me1/2 and H3K4me3 were kept without change (Fig. 6B). These results indicated that compound **14q** can inhibit LSD1 in cells. As LSD1 can promote cell migration with

diverse mechanism, for example, LSD1 may form a complex with Snail and act as a suppressor on the promoter activity of *E-cadherin*, and LSD1 can also be integrated with the SIN3A/HDAC complex and target metastasis relating genes, then the abrogation of LSD1 genetically or pharmacologically can suppress cell migration and invasion[8,31,58–60], and activity of compound **14q** against cell migration and invasion was investigated either. As the transwell and matrigel-coated transwell experiment showed in Fig. 6C and D, different concentrations of compound **14q** can suppress the migration and invasion of MGC-803 cells in a concentration-dependent manner for 24 treatments. Studies have shown that LSD1 plays a very important role in the EMT process[31,58,61,62], hence, selected biomarkers of EMT process were investigated after compound **14q** treatment. As shown in. 6E, 24 h treatment of compound **14q** leads to the accumulation of E-cadherin, the epithelial cell marker, and less amount of N-cadherin and vimentin, the mesenchymal cell marker, in a dose-dependently manner, while the amount of Snail was kept constant. All of these results indicated that compound **14q** can suppress EMT progression and inhibit cell invasion and migration in cells.

3. Conclusions

In this study, we have designed and synthesized 5-cyano-6-phenylpyrimidine derivatives containing a triazole group following FAD similarity-based designing strategy. The inhibitory activity of all compounds towards LSD1 was evaluated. SARs studies showed that compound **14q** exhibited the most potent inhibitory activity against LSD1 with IC_{50} of 183 nmol/L. With the aid of dialysis experiment, ultracentrifuge experiment and dilution assay, compound **14q** was confirmed to inhibit LSD1 in a reversible manner, further experiments also indicated that compound **14q** may inhibit LSD1 in a time-dependent manner in 30 min. Based on these findings, compound **14q** was characterized as an FAD competitive LSD1 inhibitor, and may bind LSD1 closely. Importantly, cellular experiment also indicated that compound **14q** can contribute to the accumulation of mono-, and di-methylation of H3K4 and H3K9. Furthermore, with the treatment of compound **14q**, EMT can be reversed in gastric cancer cells and cell migration and invasion ability can also be inhibited. So, our findings indicated that these 5-cyano-6-phenylpyrimidine derivatives could be served as candidates of LSD1 inhibitors for further development with FAD similarity-based designing strategy.

4. Experimental

4.1. General information

Reagent and solvent were purchased from commercial sources and were used without further purification. ^{1}H NMR and ^{13}C NMR spectra were determined on a Bruker 400 and 100 MHz spectrometer (Ettlingen, Germany), respectively. High resolution mass spectra (HRMS) were recorded on a Waters Micromass spectrometer (Milford, MA, USA) by electrospray ionization (ESI).

4.2. General procedure for the synthesis of compounds *6a–f* and *15a–d*

2-Mercapto-dihydroyrimi derivatives **4a–f** (1 mmol), propargyl bromide (1 mmol) were dissolved in dry dioxane and stirred under refluxed for 3 h. Up completion of the reaction, phosphorous oxychloride was added dropwise with stirring, the mixture was kept the temperature for 1 h, and then quenched with water. The solid was filtered off, washed with water, dried and crystallized from aqueous ethanol to yield the pure product. Compounds **15a–d** were also synthesized from compounds **4a–d** and **11** following the same procedure.

4.3. General procedure for the synthesis of compounds *9a–f* and *13a–f*

Compounds **6a**, **c–f** (5 mmol), azide derivatives **8** (5 mmol), $CuSO_4 \cdot 5H_2O$ (62 mg, 0.25 mmol), sodium ascorbate (100 mg, 0.5 mmol), THF (20 mL) and H_2O (20 mL) were added to a round-bottom flask and stirred at room temperature. TLC indicated completion of the reaction. Water was added and the reaction mixture was extracted with EtOAc. The organic layers were washed with brine, dried over anhydrous Na_2SO_4 and concentrated under vacuum, and the crude product was then further purified by recrystallized from acetone to give the pure product. Compounds **13a–f** were also synthesized from compounds **6a–f** and **12** following the same procedure.

4.4. General procedure for the synthesis of compounds *7a–g, 10a–l, 14a–w* and *16a–d*

Appropriate amine and equimolar amount of compounds **6a–f**, **9a–f, 13a–f** and **15a–d** were in the solvent of ethanol under 80 °C for 3 h. Upon completion, the precipitated product was filtered off and washed with ethanol for three times, which then recrystallized with ethanol to yield the pure product.

4.5. Cell cultures

The human gastric cancer cell line MGC-803 was obtained from Cell Bank of Shanghai Institute of Biochemistry and Cell Biology, Chinese Academy of Sciences (Shanghai, China). Cells are cultured in RPMI-1640 medium with 10% fetal bovine serum (FBS) and incubated at 37 °C and 5% CO_2.

4.6. LSD1 enzymatic assay

The inhibition of LSD1 activity by compound **14q** was evaluated according to our publication[8]. pET-28b-LSD1 (full length) was transfected into BL21 (DE). Then, the protein was induced with 0.25 μmol/L IPTG following sonication and purified with Ni-NTA (Qiagen, Tübingen, Germany), Resource Q (GE, Pittsburgh, PA, USA) and Sephacryl S-200 HR (GE, Pittsburgh, PA, USA). Then 5 nmol/L recombinant LSD1 and 25 μmol synthesized H3K4me2 peptide were incubated with the compounds with additional 50 nmol FAD, 20 nmol Amplex Red and 5.5 U/mL horseradish peroxidase for 30 min. Finally, the fluorescence intensity was read at ex 530 nm and ex 590 nm using EnVision Plate Reader (PerkinElmer, Waltham, MA, USA) to calculate the inhibition rate.

The dilution assay was performed following publication[63]. First, LSD1 recombinant was incubated compound **14q**, GSK-LSD1, or DMSO for 1 h. Then we diluted the reaction system for 80 times. Finally, the above stated method was applied to detect the activity of LSD1 before and after dilution.

In the ultrafiltration experiment, LSD1 recombinant was incubated with a concentration of 20-fold IC_{50} inhibitor. The mixture was then added to a 10 kDa cut-off ultrafiltration tube (Millipore, Darmstadt, Germany) for centrifugation to remove the

unbound compound. Finally, reversibility of the compound was evaluated by LSD1 assay for the upper chamber reaction system.

In the dialysis experiment, after incubation of the recombinant LSD1 and compound **14q** for 1 h at 37 °C, we dialyzed the reaction system against 50 mmol/L HEPES buffer (pH 8.0) for 24 h at 4 °C, and the buffer was replaced every 12 h, and the reversibility of the compounds was evaluated based on the activity of LSD1 in the dialysis tube.

For the competitive analysis, demethylase activity of LSD1 was assessed in the presence of diverse concentrations of compound at a specific concentration of histone substrate and diverse concentrations of FAD, and kinetics values were obtained using Lineweaver−Burk plots made by GraphPad 6.0.

4.7. MAO-A/B enzymatic assay

The MAO-A and -B were purchased from Active Motif (Cat#31502, Cat#31503, Carlsbad, CA, USA). Biochemical Kits were purchased from Promega (MAO-Glo Assay, Madison, WI, USA). Inhibition assay was carried out according to the manufacturer's protocol. The tested compound solution was transferred into a 384-well plate by Mantis (Formulatrix, Bedford, MA, USA) in triplicate, then incubated with 10 μL of recombinant MAO-A or -B solutions at room temperature for 15 min (the final concentration was 15 and 20 nmol/L, respectively), followed by adding 10 μL of luciferin derivative substrate (the final concentration was 10 μmol/L) to initiate the reaction. After incubation for 60 min at room temperature, the reporter luciferase detection reagent (20 μL) was added and incubated with each reaction for an additional 20 min. Relative light units (RLU) were detected using EnVision Plate Reader (PerkinElmer, Waltham, MA, USA).

4.8. Cell viability assay

The MTS method was applied to the measurement of cell proliferation according to the manufacture's instruction (Promega, Madison, WI, USA). Each treatment was performed triplicate at least.

4.9. Western blotting

Western blot was performed with the total lysates using RIPA buffer and total histone was extracted using a histone extraction kit (Epigentek, Farmingdale, NY, USA). Same amounts of protein were subjected to SDS-PAGE, and then transferred to 0.2 μm nitrocellulose membranes (PALL, Cortland, NY, USA). After blocking with 5% nonfat dry milk PBS solution, the membranes were incubated at 4 °C with respective antibody overnight, followed by incubation with a secondary antibody conjugated with horseradish peroxidase. Finally, the blot was visualized by enhanced chemiluminescence kit (Thermo Fisher, Rockford, IL, USA).

Recombinant-based thermo stability assay: LSD1 recombinant was incubated with indicated concentrations of compound for 1 h, then the mixture was heat at 53 °C using PCR instrument (SensoQuest, Göttingen, Germany) for 3 min, after incubation, the mixture was subject to Western blotting analysis.

Cellular based thermo stability assay: cells (5×10^5) were treated with indicated compound or with DMSO for 1 h, washed with PBS three times, and dissolved in 50 μL of PBS supplemented with a protease inhibitor cocktail (Roche, Mannheim, Germany), followed by heating at the indicated temperatures in a PCR instrument (SensoQuest). Treated cells were then subjected to snap-freezing in liquid nitrogen and thawed on ice for 3 cycles. The protein levels of LSD1 in equal amounts of the supernatant were examined by Western blotting. GAPDH was used as the control.

4.10. Transwell assay

For the migration assay, Costar® Transwell (Corning, Lowell, MA, USA) cell culture chamber (8.0 μm pore size for the porous membrane) was used. Cells and compounds were seeding into the upper chambers containing 1% FBS. Meanwhile, 600 μL medium with 20% FBS was used as chemoattractant in the lower chamber. After incubation for 24 h, cells passing through the membrane were quantified with high content screening using Hoechst 33,258 for cell counting.

For invasion assays, cells were placed in upper chamber coated with Matrigel (Life, Bedford, MA, USA), then the experiment was performed the same as stated above.

4.11. Statistical analyses

Data were expressed as the mean ± S.D. The significance of the difference between different groups was determined with analysis of variance (ANOVA) and Student *t* test, which was used to compare the difference between the two groups by SPSS 17.0. Results were considered statistically significant at $^{*}P < 0.05$, $^{**}P < 0.01$ was considered highly significant. Date are mean ± S.D. All experiments were carried out at least three times.

4.12. Molecular modeling studies

All molecular modeling studies were performed with MOE Version 2015.10. A number of X-ray crystal structures of LSD1 were available from the RCSB protein data bank. At the present, the highest solution crystal structure of LSD1 (PDB:2DW4) without any ligand exect its cofactor FAD was selected as the docking template. The protein was prepared with Quickprep module of MOE 2015.10 under default Amber 10:EHT forcefiled. Here, the waters expect water 1032 were deleted, the hydrogen atoms were added, and residues were protonated with pH = 7. The structures of compounds **10a** and **14q** were executed by energy minimization and conformation search. Finally, the compounds were docked into the FAD-binding active site of LSD1 by flexible docking with default parameters.

Acknowledgments

This work was supported by National Natural Science Foundation of China (Project Nos. 81430085 and 81773562 for Hongmin Liu, No. 81602961 for Yichao Zheng and No. 81703328 for Liying Ma). National Key Research Program (Nos. 2018YFE0195100 and 2016YFA0501800 for Hongmin Liu, China). Science and Technology Innovation Talents of Henan Provincial Education Department (19IRTSTHN001, China); Scientific Program of Henan Province (No. 182102310070, for Liying Ma, China).

Author contributions

Liying Ma contributed to the conceptualization and methodology. Haojie Wang contributed to the investigation, original draft

writing, review and editing. Yinghua You contributed to the validation and visualization. Chaoya Ma contributed to the software and visualization. Yuejiao Liu contributed to the formal analysis and visualization. Feifei Yang contributed to the data curation. Yichao Zheng contributed to the supervision, original draft writing, review and editing, project administration. Hongmin Liu contributed to the supervision, funding acquisition, and resources.

Conflicts of interest

The authors declare no conflicts of interests.

Appendix A. Supporting information

Supporting data to this article can be found online at https://doi.org/10.1016/j.apsb.2020.02.006.

References

1. Wu H, Deng Y, Feng Y, Long D, Ma K, Wang X, et al. Epigenetic regulation in B-cell maturation and its dysregulation in autoimmunity. *Cell Mol Immunol* 2018;**15**:676−84.
2. Jostes S, Nettersheim D, Schorle H. Epigenetic drugs and their molecular targets in testicular germ cell tumours. *Nat Rev Urol* 2019;**16**:245−59.
3. Shi Y, Lan F, Matson C, Mulligan P, Whetstine JR, Cole PA, et al. Histone demethylation mediated by the nuclear amine oxidase homolog LSD1. *Cell* 2004;**119**:941−53.
4. Kaniskan HÜ, Martini ML, Jin J. Inhibitors of protein methyltransferases and demethylases. *Chem Rev* 2018;**118**:989−1068.
5. Cho HS, Suzuki Dohmae N, Hayami S, Unoki M, Yoshimatsu M, et al. Demethylation of RB regulator MYPT1 by histone demethylase LSD1 promotes cell cycle progression in cancer cells. *Canc Res* 2011;**71**:655−60.
6. Anastas JN, Zee BM, Kalin JH, Kim M, Guo R, Alexandrescu S, et al. Re-programing Chromatin with a bifunctional LSD1/HDAC inhibitor induces therapeutic differentiation in DIPG. *Canc Cell* 2019;**36**:528−44.
7. Gelato KA, Shaikhibrahim Z, Ocker M, Haendler B. Targeting epigenetic regulators for cancer therapy: modulation of bromodomain proteins, methyltransferases, demethylases, and microRNAs. *Expert Opin Ther Targets* 2016;**20**:783−99.
8. Zheng YC, Duan YC, Ma JL, Xu RM, Zi X, Lv WL, et al. Triazole-dithiocarbamate based selective lysine specific demethylase 1 (LSD1) inactivators inhibit gastric cancer cell growth, invasion, and migration. *J Med Chem* 2013;**56**:8543−60.
9. Stewart CA, Byers LA. Altering the course of small cell lung cancer: targeting cancer stem cells *via* LSD1 inhibition. *Canc Cell* 2015;**28**:4−6.
10. Schenk T, Chen WC, Gollner S, Howell L, Jin L, Hebestreit K, et al. Inhibition of the LSD1 (KDM1A) demethylase reactivates the all-*trans*-retinoic acid differentiation pathway in acute myeloid leukemia. *Nat Med* 2012;**18**:605−11.
11. Hayami S, Kelly JD, Cho HS, Yoshimatsu M, Unoki M, Tsunoda T, et al. Overexpression of LSD1 contributes to human carcinogenesis through chromatin regulation in various cancers. *Int J Canc* 2011;**128**:574−86.
12. Schulte JH, Lim S, Schramm A, Friedrichs N, Kirfel J, Versteeg R, et al. Lysine-specific demethylase 1 is strongly expressed in poorly differentiated neuroblastoma: implications for therapy. *Canc Res* 2009;**69**:2065−71.
13. Wang Y, Zhang H, Chen YP, Sun YM, Yang F, Yu WH, et al. LSD1 is a subunit of the NuRD complex and targets the metastasis programs in breast cancer. *Cell* 2009;**138**:660−72.
14. Yu YY, Wang B, Zhang K, Lei ZJ, Guo Y, Xiao HL, et al. High expression of lysine-specific demethylase 1 correlates with poor prognosis of patients with esophageal squamous cell carcinoma. *Biochem Biophys Res Commun* 2013;**437**:192−8.
15. Lv T, Yuan D, Miao X, Lv Y, Zhan P, Shen X, et al. Over-expression of LSD1 promotes proliferation, migration and invasion in non-small cell lung cancer. *PloS One* 2012;**7**:e35065.
16. Fang Y, Liao G, Yu B. Targeting histone lysine demethylase LSD1/KDM1A as a new avenue for cancer therapy. *Curr Top Med Chem* 2019;**19**:889−91.
17. Sarno F, Papulino C, Franci G, Andersen JH, Cautain B, Melardo C, et al. 3-Chloro-*N'*-(2-hydroxybenzylidene) benzohydrazide: an LSD1-selective inhibitor and iron-chelating agent for anticancer therapy. *Front Pharmacol* 2018;**9**:1006.
18. Etani T, Naiki T, Naiki-Ito A, Suzuki T, Iida K, Nozaki S, et al. NCL1, A highly selective lysine-specific demethylase 1 inhibitor, suppresses castration-resistant prostate cancer growth *via* regulation of apoptosis and autophagy. *J Clin Med* 2019;**8**:E442.
19. Matsuda S, Baba R, Oki H, Morimoto S, Toyofuku M, Igaki S, et al. T-448, a specific inhibitor of LSD1 enzyme activity, improves learning function without causing thrombocytopenia in mice. *Neuropsychopharmacology* 2019;**44**:1505−12.
20. Li LJ, Li RZ, Wang YM. Identification of selective and reversible LSD1 inhibitors with anti-metastasis activity by high-throughput docking. *Bioorg Med Chem Lett* 2019;**29**:544−8.
21. Li Y, Tao L, Zuo ZP, Zhou Y, Qian XY, Lin YY, et al. ZY0511, a novel, potent and selective LSD1 inhibitor, exhibits anticancer activity against solid tumors *via* the DDIT4/mTOR pathway. *Canc Lett* 2019;**454**:179−90.
22. Sharma SK, Hazeldine S, Crowley ML, Hanson A, Beattie R, Varghese S, et al. Polyamine-based small molecule epigenetic modulators. *Medxhemcomm* 2012;**3**:14−21.
23. Nowotarski SL, Pachaiyappan B, Holshouser SL, Kutz CJ, Li Y, Huang Y, et al. Structure−activity study for (bis)ureidopropyl- and (bis)thioureidopropyldiamine LSD1 inhibitors with 3-5-3 and 3-6-3 carbon backbone architectures. *Bioorg Med Chem* 2015;**23**:1601−12.
24. Maes T, Carceller E, Salas J, Ortega A, Buesa C. Advances in the development of histone lysine demethylase inhibitors. *Curr Opin Pharmacol* 2015;**23**:52−60.
25. Han C, Li ZR, Hou JQ, Wang Z, Xu DQ, Xue GM, et al. Bioactivity evaluation of natural product α-mangostin as a novel xanthone-based lysine-specific demethylase 1 inhibitor to against tumor metastasis. *Bioorg Chem* 2018;**76**:415−9.
26. Lee HT, Choi MR, Doh MS, Jung KH, Chai YG. Effects of the monoamine oxidase inhibitors pargyline and tranylcypromine on cellular proliferation in human prostate cancer cells. *Oncol Rep* 2013;**30**:1587−92.
27. Alnabulsi S, Al-Hurani EA, Al-shar'i NA, El-Elimat T. Amino-carboxamide benzothiazoles as potential LSD1 hit inhibitors. Part I: computational fragment-based drug design. *J Mol Graph Model* 2019;**93**:107440.
28. Cuyas E, Gumuzio J, Lozano-Sanchez J, Carreras D, Verdura S, Llorach-Pares L, et al. Extra virgin olive oil contains a phenolic inhibitor of the histone demethylase LSD1/KDM1A. *Nutrients* 2019;**11**:E1656.
29. Li ZH, Liu XQ, Geng PF, Suo FZ, Ma JL, Yu B, et al. Discovery of [1,2,3]triazolo[4,5-*d*]pyrimidine derivatives as novel LSD1 inhibitors. *ACS Med Chem Lett* 2017;**8**:384−9.
30. Somervaille T, Salamero O, Montesinos P, Willekens C, Perez Simon JA, Pigneux, et al. Safety, phamacokinetics (PK), pharmacodynamics (PD) and preliminary activity in acute leukemia of ory-1001, a first-in-class inhibitor of lysine-specific histone demethylase 1A (LSD1/KDM1A): initial results from a first-in-human phase 1 study. *Blood* 2016;**128**:4060.
31. Zheng YC, Yu B, Chen ZS, Liu Y, Liu HM. TCPs: privileged scaffolds for identifying potent LSD1 inhibitors for cancer therapy. *Epigenomics* 2016;**8**:651−66.

32. Maes T, Molinero C, Antonijoan RM, Ferrero-Cafiero JM, Martínez-Colomer J, Mascaro C, et al. First-in-human phase I results show safety, tolerability and brain penetrance of ory-2001, an epigenetic drug targeting lsd1 and mao-B. *Alzheimer's Dementia* 2017;**13**:1573−4.
33. Hollebecque A, de Bono JS, Plummer R, Isambert N, Martin-Romano P, Baudin E, et al. Phase I study of CC-90011 in patients with advanced solid tumors and relapsed/refractory non-Hodgkin lymphoma (R/R NHL). *Ann Oncol* 2019;**30**(Suppl 1):i4−9.
34. Loo Yau H, Ettayebi I, De Carvalho DD. The cancer epigenome: exploiting its vulnerabilities for immunotherapy. *Trends Cell Biol* 2019;**29**:31−43.
35. Maes T, Mascaro C, Tirapu I, Estiarte A, Ciceri F, Lunardi S, et al. ORY-1001, a potent and selective covalent KDM1A inhibitor, for the treatment of acute leukemia. *Canc Cell* 2018;**33**:495−511.
36. Chen JY, Levant B, Jiang C, Keck TM, Newman AH, Wang S. Tranylcypromine substituted *cis*-hydroxycyclobutylnaphthamides as potent and selective dopamine D3 receptor antagonists. *J Med Chem* 2014;**57**:4962−8.
37. Prusevich P, Kalin JH, Ming SA, Basso M, Givens J, Li X, et al. A selective phenelzine analogue inhibitor of histone demethylase LSD1. *ACS Chem Biol* 2014;**9**:1284−93.
38. Schmitt ML, Hauser AT, Carlino L, Pippel M, Schulz-Fincke J, Metzger E, et al. Nonpeptidic propargylamines as inhibitors of lysine specific demethylase 1 (LSD1) with cellular activity. *J Med Chem* 2013;**56**:7334−42.
39. Kumarasinghe IR, Woster PM. Cyclic peptide inhibitors of lysine-specific demethylase 1 with improved potency identified by alanine scanning mutagenesis. *Eur J Med Chem* 2018;**148**:210−20.
40. Kumarasinghe IR, Woster PM. Synthesis and evaluation of novel cyclic peptide inhibitors of lysine-specific demethylase 1. *ACS Med Chem Lett* 2014;**5**:29−33.
41. Niwa H, Umehara T. Structural insight into inhibitors of flavin adenine dinucleotide-dependent lysine demethylases. *Epigenetics* 2017;**12**:340−52.
42. Kong X, Ouyang S, Liang Z, Lu J, Chen L, Shen B, et al. Catalytic mechanism investigation of lysine-specific demethylase 1 (LSD1): a computational study. *PloS One* 2011;**6**:e25444.
43. Ma LY, Zheng YC, Wang SQ, Wang B, Wang ZR, Pang LP, et al. Design, synthesis, and structure−activity relationship of novel LSD1 inhibitors based on pyrimidine−thiourea hybrids as potent, orally active antitumor agents. *J Med Chem* 2015;**58**:1705−16.
44. Li Z, Ding L, Li Z, Wang Z, Suo F, Shen D, et al. Development of the triazole-fused pyrimidine derivatives as highly potent and reversible inhibitors of histone lysine specific demethylase 1 (LSD1/KDM1A). *Acta Pharm Sin B* 2019;**9**:794−808.
45. Liu HM, Suo FZ, Li XB, You YH, Lv CT, Zheng CX, et al. Discovery and synthesis of novel indole derivatives-containing 3-methylenedihydrofuran-2(3*H*)-one as irreversible LSD1 inhibitors. *Eur J Med Chem* 2019;**175**:357−72.
46. Zheng YC, Shen DD, Ren M, Liu XQ, Wang ZR, Liu Y, et al. Baicalin, a natural LSD1 inhibitor. *Bioorg Chem* 2016;**69**:129−31.
47. Zheng YC, Chang J, Zhang T, Suo FZ, Chen XB, Liu Y, et al. An overview on screening methods for lysine specific demethylase 1 (LSD1) inhibitors. *Curr Med Chem* 2017;**24**:2496−504.
48. Wang S, Li ZR, Suo FZ, Yuan XH, Yu B, Liu HM. Synthesis, structure−activity relationship studies and biological characterization of new [1,2,4]triazolo[1,5-*a*]pyrimidine-based LSD1/KDM1A inhibitors. *Eur J Med Chem* 2019;**167**:388−401.
49. Li ZR, Wang S, Yang L, Yuan XH, Suo FZ, Yu B, et al. Experience-based discovery (EBD) of aryl hydrazines as new scaffolds for the development of LSD1/KDM1A inhibitors. *Eur J Med Chem* 2019;**166**:432−44.
50. Zheng YC, Yu B, Jiang GZ, Feng XJ, He PX, Chu XY, et al. Irreversible LSD1 inhibitors: application of tranylcypromine and its derivatives in cancer treatment. *Curr Top Med Chem* 2016;**16**:2179−88.
51. Ma LY, Pang LP, Wang B, Zhang M, Hu B, Xue DQ, et al. Design and synthesis of novel 1,2,3-triazole-pyrimidine hybrids as potential anticancer agents. *Eur J Med Chem* 2014;**86**:368−80.
52. Ma LY, Wang B, Pang LP, Zhang M, Wang SQ, Zheng YC, et al. Design and synthesis of novel 1,2,3-triazole-pyrimidine-urea hybrids as potential anticancer agents. *Bioorg Med Chem Lett* 2015;**25**:1124−8.
53. Wang B, Ma LY, Wang JQ, Lei ZN, Gupta P, Zhao YD, et al. Discovery of 5-cyano-6-phenylpyrimidin derivatives containing an acylurea moiety as orally bioavailable reversal agents against p-glycoprotein-mediated multidrug resistance. *J Med Chem* 2018;**61**:5988−6001.
54. Baell JB, Holloway GA. New substructure filters for removal of pan assay interference compounds (PAINS) from screening libraries and for their exclusion in bioassays. *J Med Chem* 2010;**53**:2719−40.
55. Holshouser S, Dunworth M, Murray-Stewart T, Peterson YK, Burger P, Kirkpatrick J, et al. Dual inhibitors of LSD1 and spermine oxidase. *Medchemcomm* 2019;**10**:778−90.
56. Kutz CJ, Holshouser SL, Marrow EA, Woster PM. 3,5-Diamino-1,2,4-triazoles as a novel scaffold for potent, reversible LSD1 (KDM1A) inhibitors. *Medchemcomm* 2014;**5**:1863−70.
57. Lineweaver H, Burk D. The determination of enzyme dissociation constants. *J Am Chem Soc* 1934;**56**:658−66.
58. Zheng YC, Ma J, Wang Z, Li J, Jiang B, Zhou W, et al. A systematic review of histone lysine-specific demethylase 1 and its inhibitors. *Med Res Rev* 2015;**35**:1032−71.
59. Hu X, Xiang D, Xie Y, Tao L, Zhang Y, Jin Y, et al. LSD1 suppresses invasion, migration and metastasis of luminal breast cancer cells *via* activation of GATA3 and repression of TRIM37 expression. *Oncogene* 2019;**38**:7017−34.
60. Zhang J, Zhao D, Li Q, Du X, Liu Y, Dai X, et al. Upregulation of LSD1 promotes migration and invasion in gastric cancer through facilitating EMT. *Canc Manag Res* 2019;**11**:4481−91.
61. Lin T, Ponn A, Hu X, Law BK, Lu J. Requirement of the histone demethylase LSD1 in snai1-mediated transcriptional repression during epithelial-mesenchymal transition. *Oncogene* 2010;**29**:4896−904.
62. Ferrari-Amorotti G, Fragliasso V, Esteki R, Prudente Z, Colombo MP, Calabretta B, et al. Inhibiting interactions of lysine demethylase LSD1 with snail/slug blocks cancer cell invasion. *Canc Res* 2013;**73**:235−45.
63. Willmann D, Lim S, Wetzel S, Metzger E, Jandausch A, Buettner R, et al. Impairment of prostate cancer cell growth by a selective and reversible lysine-specific demethylase 1 inhibitor. *Int J Canc* 2012;**131**:2704−9.